

Feasibility analysis of the conversion of brushed to brushless direct current motor

Pudji Irasari¹, Puji Widiyanto¹, Anwar Muqorobin¹, Muhammad Fathul Hikmawan²

¹Research Center for Energy Conversion and Conservation, National Research and Innovation Agency, Bandung, Indonesia

²Research Center for Smart Mechatronics, National Research and Innovation Agency, Bandung, Indonesia

Article Info

Article history:

Received Oct 21, 2021

Revised Aug 7, 2022

Accepted Aug 26, 2022

Keywords:

Brushed direct current motor
Brushless direct current motor
Economic analysis
Substituting rotor
Technical analysis

ABSTRACT

This paper analyzes the feasibility of converting brushed direct current (BDC) to brushless direct current (BLDC) motor by substituting the wound rotor with a permanent magnet. The aim is to overcome the low quality of rewinding of wound rotors. The conversion was performed by redesigning the motor, referring to the old stator dimensions and motor specifications. Some suitable speed control systems were also examined. Technical analysis was executed by simulating motor characteristics, covering torque-speed curve, cogging, and ripple torques. Afterward, an economic analysis was done to determine the cost of making one rotor unit and the speed control and then compare it with the price of a new BDC motor with equivalent power. The results show that the motor produces 3.6 kW, 18.86 V, 176.71 A, and 28.53 Nm at 2,460 rpm with 2 phases configuration. The maximum cogging torque is 2.9 Nm. The cost of making one rotor unit plus speed control is higher than that of a new BDC motor. These results show that it is technically feasible to convert BDC into a BLDC motor but not economically or vice versa.

This is an open access article under the [CC BY-SA](https://creativecommons.org/licenses/by-sa/4.0/) license.



Corresponding Author:

Pudji Irasari

Research Center for Energy Conversion and Conservation, National Research and Innovation Agency

St. Cisitno No. 21/154D, Bandung 40135, Indonesia

Email: pudj003@brin.go.id

1. INTRODUCTION

We can find conventional brushed direct current (BDC) motors in many applications, ranging from household appliances and robotics to transportation [1], [2]. This motor has two coils, namely the field coil on the stator and the armature coil on the rotor, connected by a mechanical contactor consisting of brushes and a commutator. Such a contact mechanism reduces the reliability and efficiency of the motor because it requires regular maintenance, thus increasing machine operating costs [3], [4]. The construction of the commutator is also complicated, with copper segments separated by insulation. Therefore, damage to the commutator or rotor winding is not as easy to repair as it does to the stator winding. It requires high technical skills or advanced tools to restore the rotor's function to its original state.

In Indonesia, wound rotor repair for small-scale motors (<5 kW) is commonly carried out by small workshops that do not have standards in their work. Based on the authors' observations and experiences, the rewinding results, mainly stator and a few rotors winding, are not as good as the factory-made windings. Even in some cases, when the motor is running, its operating temperature becomes slightly higher, possibly due to the wire quality that is not the same as the original, although the diameter is the same. Therefore, the risk of subsequent damage becomes relatively high.

However, with the decreasing price of permanent magnets and the ease of buying with various available or custom sizes, the damaged wound rotor can be substituted with a permanent magnet rotor. The

old stator can still be used because the stator of the brushless direct current (BLDC) motor is the same as that of the BDC motor. BLDC motors are preferred because of their advantages, i.e., high efficiency, low cost, robustness, and high-speed operation capability [5], [6]. In several studies, the estimation of the life of electric machines is in the range of 20-40 years and even longer if good maintenance is carried out [7], [8]. Therefore, it is still possible to replace the rotor if the operating period of the motor is only about ten years. Replacement or upgrading an older system or device with new technology or features to get better performance is known as a retrofit.

There is not much literature on retrofits directly applied to electric machines, either motors or generators. Recent studies related to retrofitting systems having electrical machine components include transportation systems, industrial machinery, and power generation systems. Several studies regarding retrofitting of transportation systems and industrial machinery are: hybrid retrofits in the power coupling arrangement, namely between the internal combustion engine and in-wheel motors without mechanical equipment but directly done by the vehicle, compared to conventional parallel hybrid electric vehicle [9], converting the combustion engine vehicle into the plug-in hybrid electric vehicle (EV) [10], upgrading gasoline cars to EV using the new powertrain [11], describing a method for transforming a vehicle's conventional drivetrain into an electrically based power unit [12], conducting a field experiment of an immobile retrofitted EV battery for grid balancing [13], suggesting to improve a shaft generator frequency converter to save fuel while operating a boat by connecting it to the primary switchboard [14], retrofitting the existing computer numerical control (CNC) machines to do modest manufacturing process by employing the Arduino platform [15], and improving the performance of a machine vision system of former tractors to make it possible to control tillage tools and enable real-time field operations [16].

Meanwhile, retrofits to the power generation system include, among others: building a new controlled diode rectifier to keep the sinusoidal input current in the power system [17], optimizing the hydropower plant control scheme through a cascaded pump back arrangement powered by hydrokinetic in the dry season [18], incorporating transmission extension and coal-fired power plants adaptable retrofits to attune to inflated infiltration of wind power [19], changing a constant speed to a variable speed hydropower plant to adapt to water head reduction due to climate change and environmental degradation [20]. The latest proposed replacing the synchronous generator with a doubly-fed induction generator by replacing the rotor components and control unit.

This paper will analyze the feasibility of converting BDC to BLDC motor to overcome the low quality of rewinding wound rotor for small-scale machines <5 kW undertaken by electric motor repair local workshops in Bandung, West Java. The BDC motor studied was used by the Marlip company; one of its products is golf cars, but the company no longer exists. Conversion is performed by redesigning the motor using a new permanent magnet rotor based on the stator dimensions and specifications displayed on the nameplate. Some proper speed controls are also investigated. Analytical and numerical simulations using finite element method magnetics (FEMM) 4.2 software are carried out to obtain torque-speed characteristics, ripple torque, and cogging torque. Furthermore, an economic analysis is done by calculating the manufacturing cost of rotor components and speed control, and the result is compared with the price of a new BDC motor with an equivalent capacity.

2. RESEARCH METHOD

The study of the conversion of BDC to BLDC motor is performed with two limitations. Firstly, the magnet's grade follows the stock availability at the time of the survey. Secondly, the economic analysis is only based on the manufacturing price of each one-speed control and rotor unit. The price of the magnet was obtained from the distributor's offers, while the rotor manufacturing process was from the workshop in the city of Bandung. The prices for the other two components, speed control and the new BDC motor, were obtained from a survey on the internet.

2.1. Motor specification

The specifications, construction, and dimensions of the stator are shown in Figures 1(a), 1(b), and 1(c), respectively. It is written on the nameplate as shown in Figure 1(a) that the motor specifications are 3 kW, 36 V, 90 A, 2,800 rpm, insulation class F, ambient temperature 40°C, and working continuously for 60 minutes. Other data from the old windings still exist, i.e., the number of turns per coil=5 or the number of phase windings $N_{ph}=10$ with a wire diameter of 7.5 mm. The length of the stator lamination is 87 mm. There is no data on the motor efficiency.

The grade of silicon steel lamination used is unknown, so it is assumed that it is non-oriented grade 50H1300, with 0.5 mm thick. The magnetic curve is needed to learn whether the motor operates on its linear or saturation zone above the knee point. The analysis is conducted based on the generated magnetomotive force \mathcal{F} expressed by [21].

$$F = N_{ph} I_a \tag{1}$$

where I_a is the phase current.

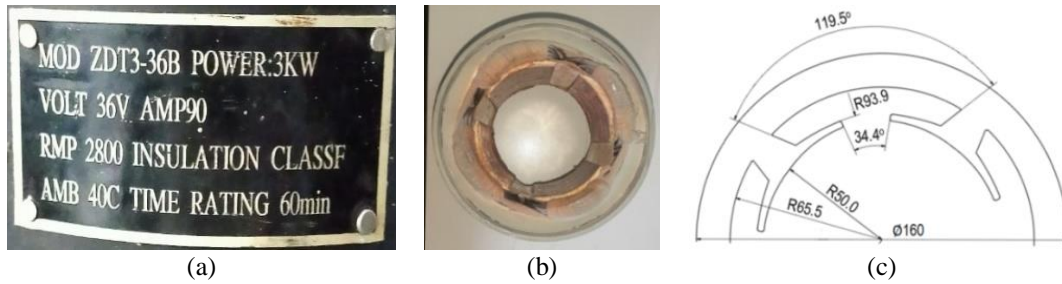


Figure 1. The studied BLDC motor (a) the nameplate, (b) the stator construction, and (c) the stator dimension

2.2. BLDC motor speed control

The speed control diagram of a BLDC motor is shown in Figure 2. A BDC motor uses a similar diagram but without a hall sensor. Speed control provides torque reference based on speed reference and speed feedback. The current delivered is proportional to the torque required to produce the speed reference.

The H-Bridge circuit is shown in Figure 3. The topology of this circuit allows forward/reverse and regenerative braking operations. To provide current in the positive direction switches S1 and S4 are closed while the negative direction is obtained by closing switches S2 and S3. The current may increase or decrease exponentially with a time constant L/R in the two cases. When the current exceeds the desired value, the bridge must be turned off by opening all the switches bridge to flow through the freewheeling diode. Alternatively, it can also be done by connecting the motor windings to the same potential node. Reversing the BDC motor's direction is by changing the current polarity. In contrast, in BLDC motors, reversing direction can be executed by changing the commutation sequence based on the hall sensor information. The number of stator slots is four as shown in Figure 1(b), so the winding can be configured as single or two phases. The selection of the number of phases will affect the speed control components.

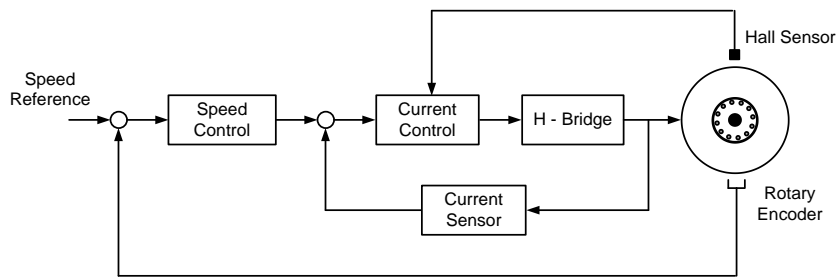


Figure 2. BLDC motor speed control diagram

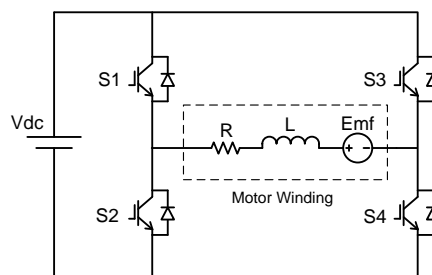


Figure 3. H-bridge circuit

2.3. Electrical parameters

The strength of the permanent magnets greatly influences the flux density in the air gap B_g , whose value is obtained from (2) [22]:

$$B_g = \frac{C_\Phi}{1 + \frac{\mu_r k_c k_{ml}}{PC}} B_r \quad (1)$$

where C_Φ is the flux concentration factor, B_r is the remanent flux density, μ_r is the relative permeability of the magnet, k_c is the Carter coefficient, k_{ml} is the magnetic leakage coefficient, and PC is the permeance coefficient, and a value in the range of 5-20 can guarantee the design's success. The greater the PC , the greater the volume of the magnet is. Therefore, in this study, PC is set at the minimum value or as close as possible to get the most economical magnet price.

In a two-phase motor, each phase, A1 and A2, work individually and produces a torque of [23],

$$T = N_{phA1} B_g L_i r_i I_{aA1} + N_{phA2} B_g L_i r_i I_{aA2} \quad (3)$$

with L_i is the stator effective length, r_i is the stator inner diameter. Since $N_{phA1} = N_{phA2}$, (3) can be rewritten as in (4).

$$T = 2N_{ph} B_g L_i r_i (I_{aA1} + I_{aA2}) \quad (4)$$

The equation (4) shows that the torque can be varied by independently adjusting the phase currents I_{aA1} and I_{aA2} . Assuming $I_{aA1} = I_{aA2} = I_a$, the torque becomes,

$$T = 4N_{ph} B_g L_i r_i I_a \quad (5)$$

If the motor winding connection is 1 phase, then the value of T drops by half.

2.4. Motor characteristics

Motor characteristics are described as torque-speed and torque-current graphs acquired using (6) and (7) [24]:

$$n_i = n_0 \left[1 - \frac{T_i}{T_0} \right] = n_0 \left[1 - \frac{I_i}{I_0} \right] \quad (62)$$

with

$$n_0 = \frac{V_{in}}{k\Phi} \quad (7)$$

where T_0 is the maximum torque, I_0 is the maximum current, T_i and I_i are the instantaneous torque, and current at the instantaneous speed n_i , V_{in} is the sum of phase A1 and A2's terminal voltage, $k = 4N_{ph}$ and $\Phi = B_g r_i \pi L_i$.

2.5. Torque ripple

Torque ripple T_r promotes bearing wear by causing vibration [25]. It can be eliminated in various ways, namely by optimizing the air gap profile, skewing the stator, skewing and optimizing the shape of the magnet, combining the slot/pole number, or adjusting pole arc to pole pitch ratio [26], [27]. Torque ripple is expressed by (8):

$$T_r = \frac{T_{max} - T_{min}}{T_{max} + T_{min}} \times 100\% \quad (8)$$

where T_{max} is the maximum torque and T_{min} is the minimum torque. In the simulation, the value of T_r is limited to about 10% or as close as possible.

2.6. Cogging torque

Cogging torque T_c is the energy variation in the air gap due to the change in reluctance \mathcal{R} between the air gap and the stator teeth [28] when the rotor rotates at an angle θ . T_c is affected by magnetic flux ϕ_m and stated with (90) [29].

$$T_c = -\frac{1}{2} \phi_m^2 \frac{d\mathcal{R}}{d\theta} \quad (9)$$

In this study, the cogging torque is simulated numerically.

2.7. Rotor components

The designed rotor component is the primary part consisting of the shaft and body. The shaft functions to transfer electromagnetic energy in the air gap into mechanical energy (rotation), while the body serves as a permanent magnet holder. The shaft material is S45C carbon steel, having a yield strength of 35 kg/mm² and tensile strength of 58 kg/mm².

The shaft will experience twisting torque and impact load during operation. In the design, the occurrence of the bending moment is also anticipated. Bending moment and impact load is predicted to occur only occasionally, and accordingly, the safety factor of bending moment δ_b (1.2-2.3) is chosen at 2. Meanwhile, the occurrence frequency of impact load is presumed relatively small, and for that consideration, the torque correction factor is taken as $K_T=1.5$. The minimum shaft diameter d_s is calculated with (10) [30]:

$$d_s = \left[\frac{5.1}{\tau_a} K_t \delta_b T \right]^{1/3} \quad (10)$$

where T is the torque obtained from (5).

2.8. Economic feasibility analysis

Economic analysis is based on the material and manufacturing costs required to make one unit of the rotor component. The manufacturing prices are obtained from one of the workshops in Bandung, West Java Province. In the final stage, the total cost of building a new rotor is compared to the price of a new BDC motor of equivalent capacity. The calculations are made in Indonesian rupiah.

3. RESULTS AND DISCUSSION

3.1. Electrical parameters and magnetic characteristics

The electrical parameters are obtained together with the dimensions of the permanent magnet, referring to the design limitations, i.e., $PC \geq 5$ and maximum ripple torque of approximately 10%. The magnet dimensions are shown in Figure 4. Diminishing the magnet thickness will decrease the power and the PC value, whereas narrowing the magnet arc will increase the torque ripple. The magnet type is neodymium magnets (NdFeB) grade N48 with $B_r=1.37$ T, $H_{cb}=1.035$ kA/m, and maximum operating temperature=80°C, selected according to the magnet manufacturer's willingness to make only one pole pair.

The selected rotor construction is a surface inset permanent magnet by considering technical and cost factors. Compared to surface permanent magnet (SPM) motors, this rotor type has a more robust mechanical structure, fewer eddy-current losses, superior field weakening capacity, and lower making costs [31]. Furthermore, the electrical parameters at the nominal frequency are listed in Table 1.

The no-load magnetic flux distribution on the stator and rotor is shown in Figure 5. The high flux density occurs at two points: the base of the stator teeth directly opposite the permanent magnets and the top of the stator teeth opposite the rotor teeth. High flux density in an area can create hot spots caused by eddy currents. Consequently, continuous motor operation for 60 minutes must be reduced in this case. Unfortunately, the type of magnet cannot be changed for the reasons described above, which is the weakness of this study.

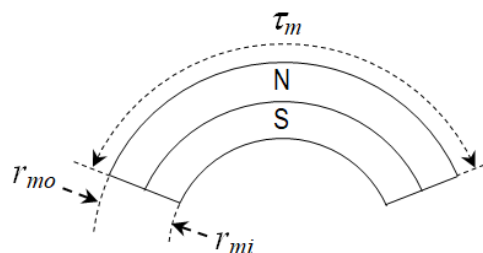


Figure 4. Magnet dimensions with outer radius $r_{mo}=0.0457$ m, inner radius $r_{mi}=0.0284$ m, and $\tau_m=0.0965$ (141°)

Table 1. The electrical parameters at a nominal frequency of 50 Hz

| Parameters, symbol | Value | Unit |
|-------------------------------|-------|-------------------|
| Air gap length, g | 4 | mm |
| Air gap flux density, B_g | 0.928 | T |
| Synchronous inductance, L_s | 0.20 | mH |
| Armature resistance, R_a | 1.59 | m Ω |
| Current density, J | 4 | A/mm ² |
| Terminal voltage, V_{in} | 18.86 | V |
| Phase current, I_a | 177 | A |
| Output torque, T | 28.53 | Nm |
| Output power, P | 3.6 | kW |
| Efficiency, η | 90 | % |

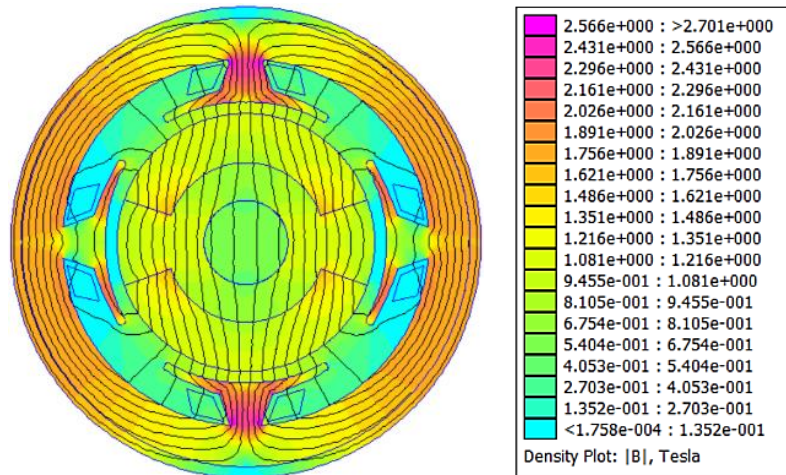


Figure 5. No-load magnetic flux distribution in the stator and rotor

Furthermore, the motor characteristics are shown in Figure 6. Figure 6(a) describes the torque-speed and current-speed curves simulated using (6)-(7) and yielding $k=40$, $\Phi=0.0127$ Wb, and $\omega_0=45.76$ rad/sec. The graphs also exhibit the continuous torque $T=28.53$ Nm occurs at $I_a=0.177$ kA, while the maximum torque $T_0=274.12$ Nm is generated at $I_0=1.70$ kA. The nominal and maximum speeds are 2460 rpm and 2746 rpm, respectively. The torque ripple obtained using (8) is 10.41%.

Then I_a , I_0 , and N_{ph} , with a length of approximately 3.93 m, are simulated to find out the operating region of the motor, and the result is depicted in Figure 6(b). It is obtained that magnetic field strength at nominal and maximum current are $H_{nom}=0.089$ kA/m and $H_{max}=3.341$ kA/m, consecutively, with the corresponding flux densities being $B_{nom}=0.897$ T and $B_{max}=1.36$ T. The value of B_g obtained using (2) is 0.928 T (at no-load current), meaning a drop of 3.36% compared to B_{nom} due to armature reaction. The motor operating region shows that it operates below the saturation curve or knee point.

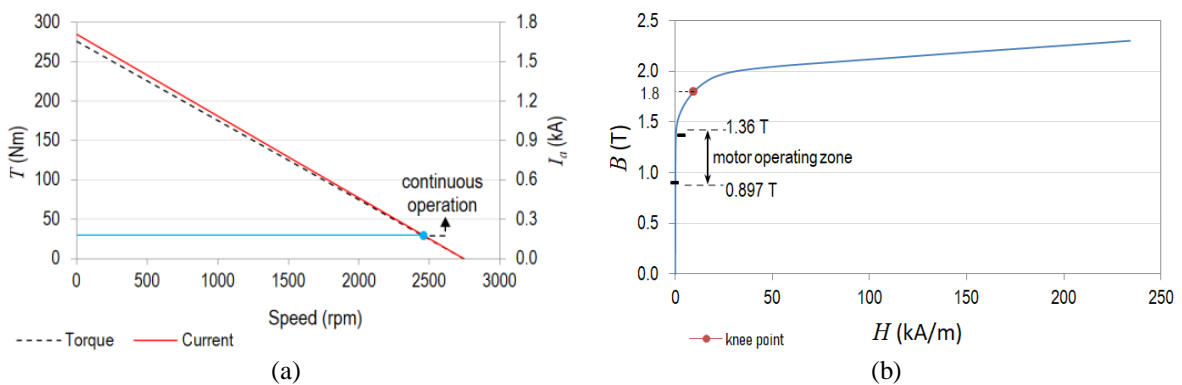


Figure 6. BLDC characteristics, (a) torque-speed graph and (b) motor operating zone

3.2. Cogging torque

Figure 7 shows the cogging torque curve with a maximum value of 2.9 Nm. In permanent magnet machines, cogging torque dominates the starting torque, compared to friction and hysteresis torque, so its value must be kept as small as possible to minimize starting current, impact load, and twisting moment on the shaft. The percentage of maximum T_c to nominal torque is 10.17%, regarded as acceptable for this study.

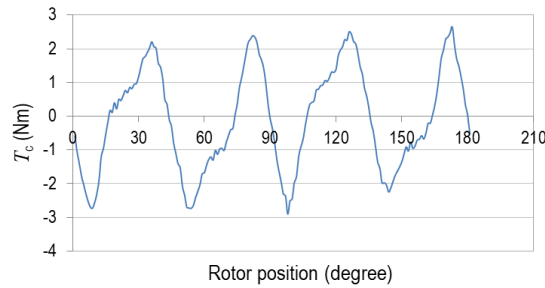


Figure 7. Cogging torque

3.3. Rotor components

The calculation result of the shaft diameter is 25 mm, according to the standard diameters of commercial bearings. Based on the d_s value and bearing load carrying capacity listed in the datasheet, the chosen bearing type is SKF 6205-RS. Figure 8 shows the design of the shaft and rotor body in the millimeter unit with the 3D shape of the stepped shaft displayed in Figure 8(a) and its detailed dimensions in Figure 8(b). The other part is the 3d shape of the rotor body with its detailed dimensions depicted in Figures 8(c) and 8(d), respectively.

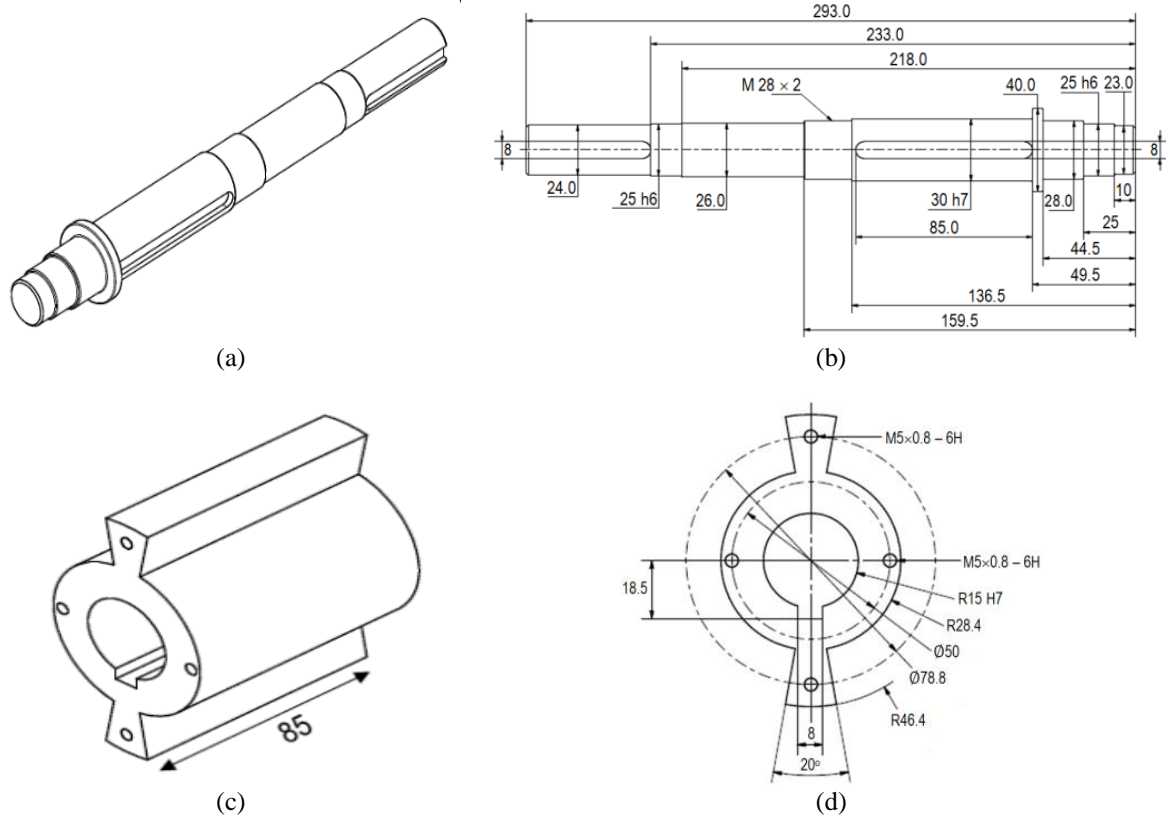


Figure 8. Rotor parts of the BLDC motor, (a) 3D shape of the shaft, (b) detailed dimensions of the shaft, (c) 3D shape of the rotor body, and (d) detailed dimensions of the rotor body

The permanent magnet assembly on the rotor is shown in Figure 9(a). It can be seen that permanent magnets cover most of the surface of the rotor body (78.3%), and the robustness of the magnet position on it only relies on magnetic attraction. It is risky that the magnets shift or get off, especially during high rotation or high load. The shift of the permanent magnet, even if only a few millimeters, can reduce the magnet area facing the active winding, namely the part of the winding in the stator slots, with an effective length of L_i . As a result, the flux linkage will decrease and ultimately reduce the output torque. In addition, the vibration due to the magnet movement when the motor is running can also cause noise. Therefore, in this study, a cylindrical cover is added to strengthen the magnet position on the rotor body as shown in Figure 9(b).



Figure 9. The permanent magnets on the rotor construction (a) without cover and (b) with cylindrical cover

3.4. Economic analysis

Material and manufacturing costs are obtained by breaking down the rotor components in Figure 9(b) into Figure 10. The part descriptions, the cost of materials, and the making of each rotor part are presented in Table 2 at an exchange rate of 1 US\$=14,263 IDR. From Table 2, it appears that the price of permanent magnets is the most dominant (76.7%) of the total rotor price. Hereafter, the total cost of making the rotor is compared with the price of a new BDC motor provided by local and foreign distributors as shown in Table 3. It is pretty knotty to convert the price of the imported motor from USD to IDR since there are cost components in the form of taxes, shipping costs, and seller profits that should be added. However, from the provided specifications, it is regarded that the two motors are identical. Hence, the price in IDR is used as a basis for comparison.

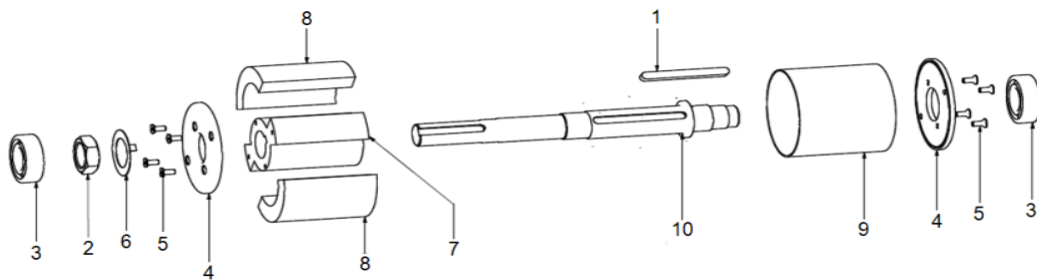


Figure 10. Decomposed rotor components

Table 2. The description and the price of the parts in Figure 7

| Part num. | Qty. | Part name | Part descriptions | Unit price | Subtotal |
|--------------|-------|--|-----------------------------|------------|-------------------|
| 1 | 1 pc | Keyway | 8×7×85, ST-37 | 100,000 | 100,000 |
| 2 | 1 pc | Hex jam nut | ANSI B18.2.4.5M-M24×3 | 50,000 | 50,000 |
| 3 | 2 pcs | Deep groove ball bearings single row with RS1 seal SKF | DIN 625 SKF-SKF 6205-RS1 | 75,000 | 50,000 |
| 4 | 2 pcs | Permanent magnet cover disc | Carbon steel, ST-37 | 165,000 | 330,000 |
| 5 | 8 pcs | Broached hexagon socket | ASME/ANSI B18.3.5M-M5×12(2) | 1,500 | 12,000 |
| 6 | 1 pc | Ring | Carbon steel, ST-37 | 103,000 | 103,000 |
| 7 | 1 pc | Rotor body | Carbon steel, ST-37 | 957,000 | 957,000 |
| 8 | 2 pcs | Permanent magnet | NdFeB grade N48 | 10,156,200 | 10,156,200 |
| 9 | 1 pc | Permanent magnet cover | Nylon | 731,000 | 731,000 |
| 10 | 1 pc | Shaft | S45C | 858,000 | 858,000 |
| Total | | | | | 13,347,200 |

Table 3. The new BDC motor price

| Procurement | Specifications | Price (USD) | Price (IDR) | Description |
|-----------------------------|---|-------------|-------------|-------------|
| Domestically available [32] | 3.7 kW, 48 V, DC motor for golf cart, brand club car, sample model for 2005 to 2010 | - | 18,000,000 | 1 unit |
| Imported from abroad [33] | Club Car 3.7 kW, 48V Electric DC motor XP-2067-S | 310 | - | 1-9 units |

It can be seen in Table 2 that the cost of making rotor components is still cheaper (25.85%) than the price of a new BDC motor. In practice, the magnet price can still be lower by downgrading it or decreasing the volume but with consequences, i.e., lower output power or higher torque ripple. Regarding the output power, it is still possible to downgrade the magnet to a certain extent until the power is down to 3 kW, which is the original motor power. As previously mentioned, the magnet price given in Table 3 is strongly influenced by the survey conditions at that time, which is the availability of the grade of the magnet material. Accordingly, the value is not fixed.

The other cost is the new speed control, which is considerably affected by the number of motor phases. When a single-phase is chosen, the main components of the speed control consist of an H-bridge circuit, a Hall sensor, a current sensor, and a speed sensor. It is similar to the required components of BDC motor speed control, except for the addition of a hall sensor whose price is less than IDR 50,000. It is very cheap compared to the price of the motor speed control Curtis for a 48 V, 325 A DC motor, which is IDR 2.6 million [34]. So, for 1 phase configuration, the speed control plus permanent magnet rotor price is IDR 13,397,200; cheaper than a new BDC motor. Nevertheless, the nominal torque of the motor is halved.

On the other hand, when choosing a BLDC motor with a two-phase configuration, we need double the motor speed control components, which means a double price is required. In this case, the available three-phase BLDC speed control price of IDR 5.2 million is taken as a reference [35]. Three-phase BLDC motor needs fewer switching components compared to a two-phase BLDC motor. As a result, the speed control price for a two-phase BLCD motor will become higher than three-phase BLDC motor speed control. Thus, the price of the rotor plus the speed control is greater than that of a new BDC motor.

4. CONCLUSION

This paper has analyzed the feasibility of converting BDC to BLDC motor viewed from technical and economic terms. With the given restrictions, the motor has nominal specifications of 2 phases, 3.6 kW, 18.86 V, 176.71 A, 28.53 Nm, and 2460 rpm. The maximum cogging torque is 2.9 Nm. Meanwhile, from an economic perspective, it is learned that the price of a permanent magnet rotor and speed control is higher than that of a new BDC motor. From the results, it can be concluded that the conversion of BDC to BLDC motor is technically feasible but not economically or vice versa.

ACKNOWLEDGEMENTS

We thank the Research Center for Energy Conversion and Conservation, The National Research and Innovation Agency, Indonesia, for all facility support, Prof. Dr. Sri Yudawati Cahyarini for most of the publication fund, and the Ngombol Teknik workshop for providing the data-related manufacturing process.

REFERENCES

- [1] D. A. Barkas, G. C. Ioannidis, C. S. Psomopoulos, S. D. Kaminaris, and G. A. Vokas, "Brushed DC motor drives for industrial and automobile applications with emphasis on control techniques: a comprehensive review," *Electronics*, vol. 9, no. 6, May 2020, doi: 10.3390/electronics9060887.
- [2] G. A. Sziki *et al.*, "Experimental investigation of a series wound DC motor for modeling purpose in electric vehicles and mechatronics systems," *Measurement*, vol. 109, pp. 111–118, Oct. 2017, doi: 10.1016/j.measurement.2017.05.055.
- [3] M. N. Ibrahim, H. Rezk, M. Al-Dhaifallah, and P. Sergeant, "Solar array fed synchronous reluctance motor driven water pump: an improved performance under partial shading conditions," *IEEE Access*, vol. 7, pp. 77100–77115, 2019, doi: 10.1109/ACCESS.2019.2922358.
- [4] S. Arunkumar and S. Thangavel, "A review paper on torque ripple reduction in brushless DC motor drives with different multilevel inverter topology," *TELKOMNIKA Indonesian Journal of Electrical Engineering*, vol. 13, no. 1, pp. 65–75, Jan. 2015, doi: 10.11591/telkomnika.v13i1.6904.
- [5] W. Lee, J. H. Kim, W. Choi, and B. Sarioglu, "Torque ripple minimization control technique of high-speed single-phase brushless DC motor for electric turbocharger," *IEEE Transactions on Vehicular Technology*, vol. 67, no. 11, pp. 10357–10365, Nov. 2018, doi: 10.1109/TVT.2018.2866779.
- [6] J. Mostafapour, J. Reshadat, and M. Farsadi, "Improved rotor speed brushless DC motor using fuzzy controller," *Indonesian Journal of Electrical Engineering and Informatics (IJEI)*, vol. 3, no. 2, Jun. 2015, doi: 10.11591/ijeie.v3i2.147.
- [7] M. S. H. Lipu and T. F. Karim, "Energy efficiency opportunities and savings potential for electric motor and its impact on GHG emissions reduction," *International Journal of Electrical and Computer Engineering (IJECE)*, vol. 3, no. 4, pp. 533–542, 2013.

- [8] O. Barré and B. Napame, "The insulation for machines having a high lifespan expectancy, design, tests and acceptance criteria issues," *Machines*, vol. 5, no. 1, Feb. 2017, doi: 10.3390/machines5010007.
- [9] S. A. Zulkifli, S. Mohd, N. Saad, and A. R. A. Aziz, "Operation and control of split-parallel, through-the-road hybrid electric vehicle with in-wheel motors," *International Journal of Automotive and Mechanical Engineering*, vol. 11, pp. 2793–2808, Jun. 2015, doi: 10.15282/ijame.11.2015.54.0235.
- [10] P. K. Gujarathi, V. A. Shah, and M. M. Lokhande, "Cost analysis for conversion of conventional vehicle into plug-in hybrid electric vehicle," *Journal of Green Engineering*, vol. 8, no. 4, pp. 497–518, 2018, doi: 10.13052/jge1904-4720.843.
- [11] R. Lairenlakpam, R. Lairenlakpam, P. Kumar, P. Kumar, G. D. Thakre, and G. D. Thakre, "Experimental investigation of electric vehicle performance and energy consumption on chassis dynamometer using drive cycle analysis," *SAE International Journal of Sustainable Transportation, Energy, Environment, and Policy*, vol. 1, no. 1, Dec. 2019, doi: 10.4271/13-01-01-0002.
- [12] K. B. Patar, P. Kumar RH, R. R. K. Jain, and S. Pati, "Methodology for retrofitting electric power train in conventional powertrain-based three wheeler," *Journal of applied research on industrial engineering*, vol. 5, no. 3, pp. 263–270, 2018.
- [13] B. Faessler, P. Kepplinger, and J. Petrasch, "Field testing of repurposed electric vehicle batteries for price-driven grid balancing," *Journal of Energy Storage*, vol. 21, pp. 40–47, Feb. 2019, doi: 10.1016/j.est.2018.10.010.
- [14] H. Schøyen and H. Sow, "A decision making tool concerning retrofit of shaft generator frequency converter," *Ocean Engineering*, vol. 109, pp. 103–112, Nov. 2015, doi: 10.1016/j.oceaneng.2015.09.003.
- [15] A. Quatrano, S. De, Z. B. Rivera, and D. Guida, "Development and implementation of a control system for a retrofitted CNC machine by using Arduino," *FME Transaction*, vol. 45, no. 4, pp. 565–571, 2017, doi: 10.5937/fmet1704565Q.
- [16] F. Pallottino *et al.*, "Machine vision retrofit system for mechanical weed control in precision agriculture applications," *Sustainability*, vol. 10, no. 7, Jun. 2018, doi: 10.3390/su10072209.
- [17] K. V. Bindu and B. J. Rabi, "A novel power factor correction rectifier for enhancing power quality," *International Journal of Power Electronics and Drive Systems (IJPEDS)*, vol. 6, no. 4, pp. 772–780, Dec. 2015, doi: 10.11591/ijpeds.v6.i4.pp772-780.
- [18] F. Wamalwa, S. Sichilalu, and X. Xia, "Optimal control of conventional hydropower plant retrofitted with a cascaded pumpback system powered by an on-site hydrokinetic system," *Energy Conversion and Management*, vol. 132, pp. 438–451, Jan. 2017, doi: 10.1016/j.enconman.2016.11.049.
- [19] Y. Wang, S. Lou, Y. Wu, and S. Wang, "Flexible operation of retrofitted coal-fired power plants to reduce wind curtailment considering thermal energy storage," *IEEE Transactions on Power Systems*, vol. 35, no. 2, pp. 1178–1187, Mar. 2020, doi: 10.1109/TPWRS.2019.2940725.
- [20] E. Bortoni *et al.*, "The benefits of variable speed operation in hydropower plants driven by Francis turbines," *Energies*, vol. 12, no. 19, Sep. 2019, doi: 10.3390/en12193719.
- [21] J. Soleimani, A. Ejlali, and M. Moradkhani, "Transverse flux permanent magnet generator design and optimization using response surface methodology applied in direct drive variable speed wind turbine system," *Periodicals of Engineering and Natural Sciences (PEN)*, vol. 7, no. 1, Feb. 2019, doi: 10.21533/pen.v7i1.230.
- [22] M. Comanescu, A. Keyhani, and Min Dai, "Design and analysis of 42-v permanent-magnet generator for automotive applications," *IEEE Transactions on Energy Conversion*, vol. 18, no. 1, pp. 107–112, Mar. 2003, doi: 10.1109/TEC.2002.808380.
- [23] J. R. Hendershot and T. J. E. Miller, *Design of brushless permanent-magnet machines*. Motor Design Books Venice, FL, USA, 2010.
- [24] K. Krykowski, J. Hetmańczyk, and D. Makiela, "Impact of windings switching on torque-speed curves of PM BLDC motor," *COMPEL-The international journal for computation and mathematics in electrical and electronic engineering*, vol. 32, no. 4, pp. 1300–1314, Jul. 2013, doi: 10.1108/03321641311317112.
- [25] S.-K. Lee, G.-H. Kang, and J. Hur, "Finite element computation of magnetic vibration sources in 100 kW two fractional-slot interior permanent magnet machines for ship," *IEEE Transactions on Magnetics*, vol. 48, no. 2, pp. 867–870, Feb. 2012, doi: 10.1109/TMAG.2011.2176323.
- [26] J. Liang, A. Parsapour, Z. Yang, C. Caicedo-Narvaez, M. Moallem, and B. Fahimi, "Optimization of air-gap profile in interior permanent-magnet synchronous motors for torque ripple mitigation," *IEEE Transactions on Transportation Electrification*, vol. 5, no. 1, pp. 118–125, Mar. 2019, doi: 10.1109/TTE.2019.2893734.
- [27] D. Wang, X. Wang, and S.-Y. Jung, "Cogging torque minimization and torque ripple suppression in surface-mounted permanent magnet synchronous machines using different magnet widths," *IEEE Transactions on Magnetics*, vol. 49, no. 5, pp. 2295–2298, May 2013, doi: 10.1109/TMAG.2013.2242454.
- [28] M. A. Noyal Doss, S. Vijayakumar, A. J. Mohideen, K. S. Kannan, N. D. B. Sairam, and K. Karthik, "Reduction in cogging torque and flux per pole in BLDC motor by adapting u-clamped magnetic poles," *International Journal of Power Electronics and Drive Systems (IJPEDS)*, vol. 8, no. 1, pp. 297–304, Mar. 2017, doi: 10.11591/ijpeds.v8.i1.pp297-304.
- [29] M. García-Gracia, Á. Jiménez Romero, J. Herrero Ciudad, and S. Martín Arroyo, "Cogging torque reduction based on a new pre-slot technique for a small wind generator," *Energies*, vol. 11, no. 11, Nov. 2018, doi: 10.3390/en11113219.
- [30] A. H. Budiarto, A. Winarno, and P. D. Setyorini, "Inventory shaft and propeller of traditional vessels in Gresik-East Java," *IOP Conference Series: Earth and Environmental Science*, vol. 750, no. 1, May 2021, doi: 10.1088/1755-1315/750/1/012061.
- [31] W. Zhao, T. A. Lipo, and B. Kwon, "Optimal design of a novel asymmetrical rotor structure to obtain torque and efficiency improvement in surface inset PM motors," *IEEE Transactions on Magnetics*, vol. 51, no. 3, pp. 1–4, Mar. 2015, doi: 10.1109/TMAG.2014.2362146.
- [32] R. Solihin, "DC motor mobil golf merk club car," *Bukalapak*. <https://www.bukalapak.com/p/mobil-part-dan-aksesoris/mesin-mobil/turbo-parts/3a6cs80-jual-dc-motor-mobil-golf-merk-club-car> (accessed Aug. 09, 2021).
- [33] Hefei Huanxin Technology Development, "Club car 3.7KW 48V electric DC motor XP-2067-S," *Alibaba*. https://www.alibaba.com/product-detail/Club-Car-3-7KW-48V-Electric_60624537573.html (accessed Aug. 09, 2021).
- [34] Hefei Huanke Electric Vehicle Parts, "China supply original forklift parts curtis series 48 V 325 A DC motor controller 1204M-5305," *Alibaba*. https://www.alibaba.com/product-detail/China-supply-original-Forklift-Parts-curtis_60265522806.html (accessed May 05, 2022).
- [35] Jinan Keya Electron Science and Technology, "High current 300 A 400 A brushless DC controller 48 V 3 kW 4 kW BLDC motor speed controller," *Alibaba*. https://www.alibaba.com/product-detail/high-current-300A-400A-Brushless-dc_60831750256.html (accessed May 05, 2022).

BIOGRAPHIES OF AUTHORS

Pudji Irasari    completed B.Eng. degree in Universitas Brawijaya in 1994 and M.Sc. degree at Oldenburg University, Germany in 2003. Her research interests include analysis of renewable energy power system, electric machine design, and electrical power system assessment. She is currently conducting a low head hydropower systems project at the Research Center for Energy Conversion and Conservation, The National Research and Innovation Agency (BRIN), Indonesia. She can be contacted at email: pudj003@brin.go.id or pirasari@yahoo.com.



Puji Widiyanto    received his B. Eng. and M. Eng. degrees both in Mechanical Engineering, first in STT Mandala and later in Institute Technology Bandung, Indonesia. Having focused his research on the structure and mechanical design of electrical machines, he is now working as a researcher at the Research Center for Energy Conversion and Conservation, The National Research and Innovation Agency (BRIN). Currently, he is conducting a project on low head hydropower system. He can be contacted at email: puji010@brin.go.id or pujiwidiyanto@gmail.com.



Anwar Muqorobin    was born in Temanggung, Indonesia in 1977. He received the bachelor degree from Universitas Diponegoro in 2001, the master degree from Institut Teknologi Bandung in 2013, and the doctoral degree from Institut Teknologi Bandung in 2019, all in Electrical Engineering. He is currently a researcher at Research Center for Energy Conversion and Conservation, The National Research and Innovation Agency (BRIN). His research interest is inverter. He can be contacted at email: anwa014@brin.go.id or anwa006@gmail.com.



Muhammad Fathul Hikmawan    received his B. Eng. and M. Eng. degrees both in Mechanical Engineering, first in STT Mandala and later in Institute Technology Bandung. Having focused his research on the mechanical design and manufacture of electrical machines. He is now working as a researcher at the Research Center for Smart Mechatronics, The National Research and Innovation Agency (BRIN). He can be contacted at email: fathul muha103@brin.go.id.